tvst

DOI: 10.1167/tvst.4.3.7

Article

Refined Frequency Doubling Perimetry Analysis Reaffirms Central Nervous System Control of Chronic Glaucomatous Neurodegeneration

Matthew A. Reilly[1] ✉, Analaura Villarreal[1] ✉, Ted Maddess[2] ✉, and William Eric Sponsel[1-4]

[1] Biomedical Engineering, University of Texas at San Antonio (UTSA), San Antonio, TX, USA
[2] Australian Research Council Centre of Excellence in Vision Science, Canberra, Australia
[3] Baptist Medical Center WESMDPA Glaucoma Service, San Antonio, TX, USA
[4] Rosenberg School of Optometry UIW, San Antonio, TX, USA

Correspondence: William Eric Sponsel, Suite 306 Madison Square Building, 311 Camden Street, San Antonio, TX 78215, USA. e-mail: sponsel@earthlink.net

Received: 1 November 2014
Accepted: 19 April 2015
Published: 8 June 2015

Keywords: refined data analysis; glaucoma; neuroprotection; neurodegeneration; visual fields; perimetry; frequency doubling; jigsaw effect

Citation: Reilly MA, Villarreal A, Maddess T, Sponsel WE. Refined frequency doubling perimetry analysis reaffirms central nervous system control of chronic glaucomatous neurodegeneration. Trans Vis Sci Tech. 2015;4(3):7, doi:10.1167/tvst.4.3.7

Purpose: Refined analysis of frequency doubling perimetric data was performed to assess binocular visual field conservation in patients with comparable degrees of bilateral glaucomatous damage, to determine whether unilateral visual field loss is random, anatomically symmetric, or non-random in relation to the fellow eye.

Methods: Case control study of 41 consecutive patients with bilaterally mild to severe glaucoma; each right eye visual field locus was paired with randomly-selected co-isopteric left eye loci, performing 690,000 (10,000 complete sets of 69 loci) such iterations per subject. The potential role of anatomic symmetry in bilateral visual field conservation was also assessed by pairing mirror-image loci of the right- and left-eye fields. The mean values of the random co-isopteric and the symmetric mirror pairings were compared with natural point-for-point pairings of the two eyes by paired *t*-test.

Results: Mean unilateral Matrix threshold across the entire 30-degree visual field were 17.0 dB left and 18.4 dB right (average 17.7). The better of the naturally paired concomitant loci yielded binocular equivalent mean bilateral Matrix threshold of 20.9 dB, 1.6 dB higher than the population mean of the 690,000 coisopteric pairings ($t = -10.4$; $P < 10^{-12}$). Thus, a remarkable natural tendency for conservation of the binocular Matrix visual field was confirmed, far stronger than explicable by random chance. Symmetric pairings of precise mirror-image loci also produced values higher than random co-isopteric pairings (Δ 1.1 dB; $t = -4.0$; $P = 0.0004$).

Conclusions: Refined data analysis of paired Matrix visual fields confirms the existence of a natural optimization of binocular visual function in severe bilateral glaucoma via interlocking fields that could only be created by CNS involvement. The disparity of paired Matrix threshold values at mirror-image loci was also highly nonrandom and quantitatively inverse from the expected if anatomic symmetry factors were merely passively contributing systematically to the compensatory binocular Matrix effect.

Translational Relevance: The paired eyes and brain are reaffirmed to function as a unified system in the progressive age-related neurodegenerative condition chronic open angle glaucoma, maximizing the binocular visual field. Given the extensive homology of this disorder with other age-related neurodegenerations, it is reasonable to assume that the brain will similarly resist simultaneous bilateral loss of paired functional zones in both hemispheres in diseases like Alzheimer's and Parkinson's disease. Glaucomatous eyes at all stages of the disease appear to provide a highly accessible paired-organ study model for developing therapeutics to optimize conservation of function in neurodegenerative disorders.

Introduction

In chronic glaucoma diffuse damage occurs in about 55% of fields.[1] This may be attributable to global mechanisms like oxidative damage.[2,3] About 34% of glaucomatous fields display nasal steps, and 57% arcuate scotomas.[1] These are primarily the result of damage around the margin of the optic disc. We have recently reported that the fields obtained in late stage glaucoma appear to be strongly determined by a centrally driven binocular process.[4] The process appears to maintain binocular patency of late stage fields.

Other studies support the possibility that glaucomatous neurodegeneration may be partially under central nervous system (CNS) control. Studies of the DBA/2 mouse model of glaucoma report dieback of retinal ganglion cell (RGC) axons from the superior colliculus (SC),[5,6] following reduction in axoplasmic transport. Evidence of dieback from the lateral geniculate nucleus (LGN) is less clear in primate experimental glaucoma, but both LGN and striate cortical cell death[7,8] and shrinkage[7,9] have been reported. Excellent reviews of the dieback mechanisms have been published.[10,11] Both the SC and cortex show binocular interaction and so both provide potential substrates for mechanisms that govern binocular visual field (VF) patency in late glaucoma. Although there might be an active process trying to maintain binocular patency in late stage disease, it is also possible that there is some form of passive winner-take-all competition for resources between dichoptic afferents leading to one eye dominating within a patch of the CNS, and so too, a patch of the VFs. Interestingly if the striate cortex is also involved, then this brings in the prospect that the range of interactions of the (active or passive) process might be expected to minimally involve a left (L) and right (R) eye dominance columns, or perhaps a LRL or RLR sandwich of adjacent columns. Figure 1 shows the projection of human ocular dominance columns into visual space.[12] The width of patches seen by LRL/RLR sandwiches is about the smallest size of field regions showing binocular patency.[4] Note that from about 10 degrees eccentricity and beyond the columns tend to extend along arcs of polar angle; thus binocular cortical influences could also contribute to arcuate scotomas characteristic of chronic glaucoma.

The issue then arises: is the striate cortex involved or is everything determined in the SC as in mice? Our previous study used fields of 47 late stage glaucoma patients measured using standard automated perimetry (SAP). Here we have reproduced that study but used the Matrix perimeter, which employs spatial frequency doubling (FD) stimuli. These stimuli have very low spatial frequencies. This brings in another aspect of cortical processing, binocular symmetry. Binocular symmetry is sensed within a part of the central VF that grows much larger as the spatial frequency content of the stimuli gets lower.[13,14] There is an anatomical substrate for this in the form of trans-collosal reciprocal connections between the parts of V2 representing the central VF.[15] Thus, if the cortex were involved, one might expect something different in terms of the binocular interactions within the central VFs when low spatial frequency stimuli are employed, since the fates of cells sensitive to low spatial frequencies might be different. Sensitivity to binocular symmetry for small stimuli like those used in SAP is only expressed in the central few degrees of the field, and so would not be captured by SAP fields. Thus we might expect some differences between our earlier SAP results and those obtained with FD stimuli.

This study mimics our previous study that used SAP stimuli in a larger set of glaucoma patients with predominantly severe disease, but the present FD cohort includes individuals with mild and moderate bilateral glaucoma as well. The first objective was to evaluate whether binocular patency is again preserved. The secondary objective was to identify potential differences between SAP and Matrix fields that might suggest the influence of the striate cortex rather than the SC, particularly within the central field.

Methods

Institutional review board (IRB)/ethics committee approval was obtained for this Health Insurance Portability and Accountability Act (HIPAA)-compliant cross-sectional study, which was fully adherent to the tenets of the Declaration of Helsinki. All available records for patients with bilateral chronic progressive glaucoma in the IRB-sanctioned San Antonio, Texas, glaucoma subspecialty clinic were assessed, and all patients meeting the inclusion criteria are included in this analysis. Inclusion criteria were: (1) perimetric experience (two or more prior VFs) and reliability (false-positive and false-negative rates both $<25\%$) with comparable degrees of mild, moderate, or severe VF loss in both eyes using Matrix (Carl Zeiss Meditec; Dublin, CA) Frequency Doubling Technology (FDT) perimetry. The FDT Matrix pattern employs 69 (17 loci per quadrant and one central

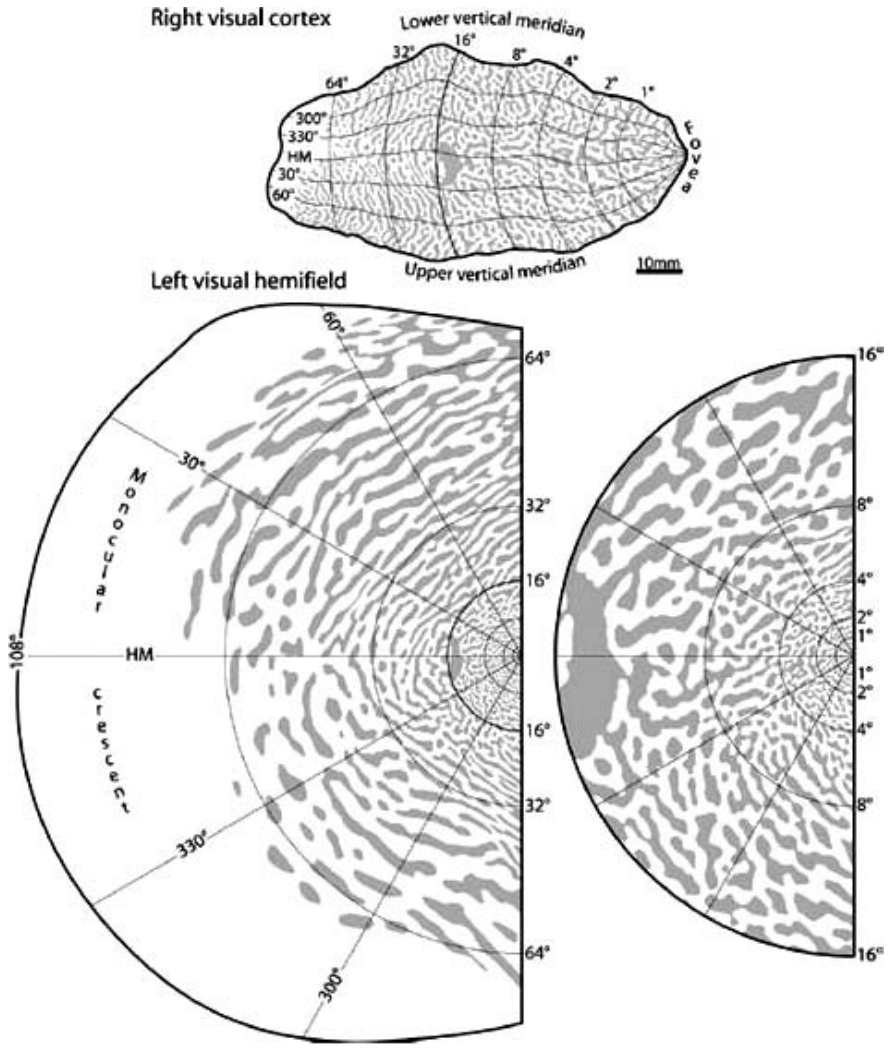

Figure 1. Projection of human ocular dominance columns onto the VF. *Top*: The retinotopic map superimposed on the pattern of ocular dominance columns for a right visual cortex. *Bottom left*: The projection of the column pattern onto the visual hemifield. *Bottom right*: The central 16 degrees. Note that the amount of VF represented by the columns changes with eccentricity. Reproduced with permission from Adams, Sincich, and Horton, 2007.[12]

locus) $5° \times 5°$ square targets across a 30-degree central VF reversing sinusoidal contrast gratings of spatial frequency of 0.5 cycles/degree at a counterphase flicker temporal frequency of 18 Hz. These produce the FD percept across the field.[16] A Bayesian threshold estimation strategy is applied to provide thresholds with normal attenuation values numerically comparable to those attained using standard forms of static perimetry.[17] VF loss is typically seen at an earlier clinical stage with Matrix than with more traditional automated static perimetry that utilize focal light stimuli flashed for 0.2 seconds in an illuminated bowl (as used in our prior study). Included in this study were all patients meeting reliability criteria exhibiting comparable degrees of VF loss in both eyes (using previously published full-threshold scoring criteria; see below),[18–20] (2) visual acuity $\geq$ 20/80 in both eyes, (3) with moderate to severe excavatory optic neuropathy (cup/disc ratio $\geq$0.5 in both eyes), and (4) bilaterally stable intraocular pressure in both eyes in the range 6 to 16 mmHg.

Briefly outlined, the study design is as follows:

1. Objective scoring of bilaterally reliable stable glaucoma patient VFs into mild, moderate, and severe Humphrey Visual Field Analyser (HVFA) II VF chart data screening confirmed reliable for paired eyes with bilateral defects within the same grading category or within one step thereof;
2. Criteria met: Document bilateral VF data mean

deviation (MD) and pattern standard deviation (PSD) oculus uterque (both eyes; OU) and calculate maximal concomitant threshold values OU;
3. Perform refined data analysis with 10,000 iterations of optionally equivalent bilateral co-isopteric outcomes for each subject;
4. Perform bilateral absolute symmetry analysis for each of the 69 points on the FDT analyses OU; and
5. Calculate the paired *t*-test *P* values for all comparisons (i.e., mean right and left eye versus computed and actual bilateral binocular VF values).

Details of each step are described further below.

A majority of participants had both FDT and Humphrey VFA II VFs, and when both were available glaucoma severity was defined using the latter. In those with only FDT fields an adapted version of a previously published algorithm[19] intended to produce concordance between HVFA II and Matrix FDT pathologic categories was applied. Severe VF loss was defined as Humphrey MD worse than −12 dB, and/or 37 or more points depressed at or below 5%, and or 20 or more below 1%, and/or a glaucomatous scotoma with one or more pericentral loci at 0 dB or two such loci at or below 15 dB. Moderate VF loss was defined as having a MD between −12 and −6 dB, and/or 18 to 36 points depressed at or below 5%, and/or 10 to 19 points depressed at or below 1%, and no points in the central 5 degrees at 0 dB, and no pericentral hemifield pairs at or below 15 dB. Mild VF loss was defined as having MD > −6 dB and between 7 and 17 points depressed below 5%, and 10 or fewer points depressed at or below 1%, and no points in the central 5 degrees at 0 dB, and no hemifield pairs in the central 5 degrees at or below 15 dB.

All eyes were tested with best refractive lens correction in place during a single perimetric session. All patients with evidence of ptosis underwent perimetric testing with the upper lid taped to the brow to avoid lid artifact. Prior work demonstrated the predictability of the binocular VF via pairing of directly corresponding (concomitant) loci of the individual right and left eye VFs.[21] For the present statistical analysis, to assess the randomness of the contribution of each eye to binocular visual function, each left eye Matrix 30-2 VF locus was paired with (α) its actual corresponding (concomitant) right eye locus, or (β) multiple random co-isopteric right eye loci having equal eccentricity from fixation (Fig. 2). This was performed in a sequential manner choosing one random co-isopteric left eye locus for each right eye locus until all 69 were paired, repeating this process 10,000 times for all 41 paired VFs. The per-locus maximum light-sensitivity threshold values for all 69 loci within the central 30 degrees for all subjects were then generated, for measured contralateral concomitant pairings and for physiologically balanced alternative pairings, using combinations α and β, above. As an additional exercise to estimate the optimal field pairing that could be obtained from the two eyes, the maximum field mean of all 10,000 randomized binocular fields was also determined for each of the 41 subjects. Mean and maximum light attenuation threshold results were then compiled for each subject to provide means of each for all 41 subjects. The results for each patient were fitted with an extreme value probability density function. Composite means for the study population were then compared by paired *t*-test.[4]

Additional comparisons were made pairing each left eye VF locus with its horizontal mirror-image locus from the right eye (χ) to determine the potential contribution of anatomic symmetry. To identify the extent of any such passive anatomic compensation, probability distribution comparisons were performed to determine to what extent passive bilateral symmetry might account for any observed optimization of binocular visual function. Heat maps of the higher paired threshold value projected binocular VF were created for all subjects for combinations α, β, and χ, to compare with one another and with their associated individual right and left eye 3-D projections. All computations were carried out using MATLAB version 7.13 (The Mathworks, Inc.; Natick, MA) in the University of Texas at San Antonio Department of Biomedical Engineering. It should be emphasized that all probability values presented are the result of comparisons of the final refined data compilations of each of the 41 individuals in the study, and there is no statistical retreatment of any nonindependent variables in this analysis.

An additional analysis was applied to the central VF to identify cortical effects in preserving the central binocular field. Loci located within a central, vertically oriented ellipse with major radius 15° and minor radius 10° from fixation were compared using the same tests for randomization and mirror-like anatomical symmetry as above. This analysis was also repeated for points outside this central ellipse.

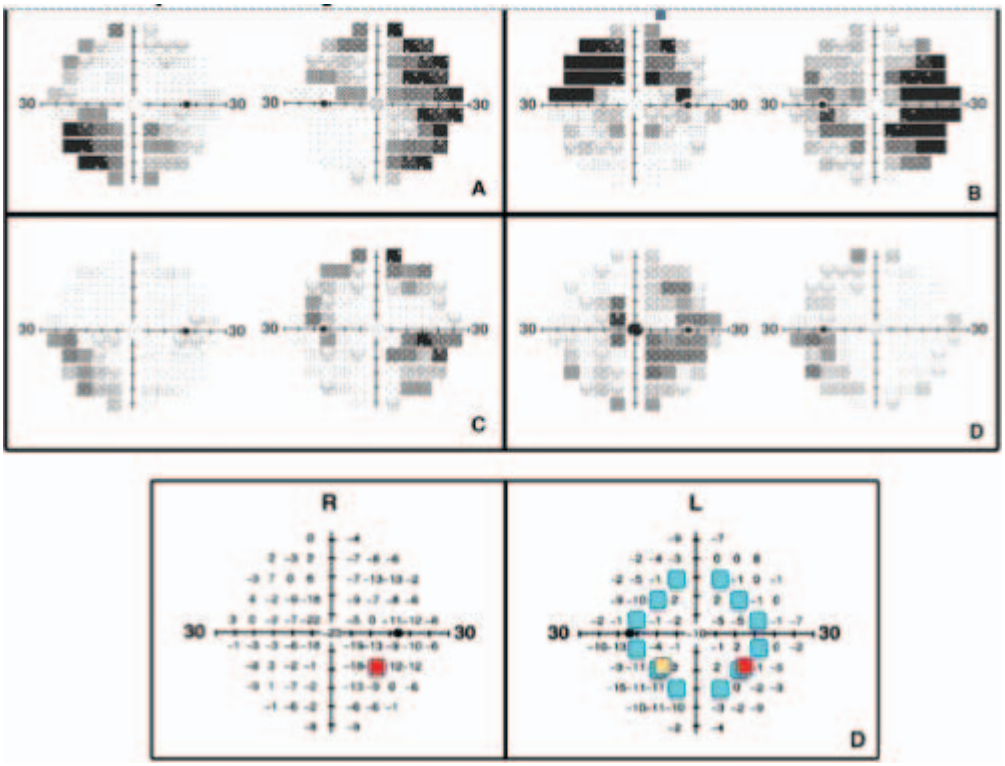

Figure 2. Specimen VF pairs and analytical algorithm. Gray scale (*above*) and pairing algorithm (*below*) representations of FDT 30-2 VF plots. The four gray-scale VF plots show the paired right and left eye VFs of 4 of the 41 study subjects with clinically stable bilaterally advanced chronic glaucoma. Note the complementarity of the patterns of the focal areas of visual loss and visual conservation between the paired eyes, providing compensation when both eyes are used together to view the binocular VF. The pairing algorithm used matched each of the 69 loci in the left VF (*lower left*) with (α) the corresponding locus of the right VF (red), (β) any one randomly selected point from among those equidistant from central fixation (teal), and (χ) the precise mirror-image locus (orange).

Results

This study evaluated all 41 adult patients meeting the inclusion criteria. Their mean age was 68 ± 2 [SEM] years. Thirty were female, and 11 were male. Their mean cup/disc ratio values were 0.72 ± 0.03 in the right eye and 0.73 ± 0.03 in the left. Their mean FDT Matrix 30-2 MD and PSD values were −11.16 and 5.79, respectively, for left eyes and −10.89 and 6.2 for right eyes (see Table 1). The age, gender, and all right and left eye MD and PSD values for the 41 subjects are provided in Table 2. Twelve subjects had severe VF loss in both eyes, seven had moderate loss in both eyes, seven had mild loss in both eyes, eight had severe loss in one eye and moderate loss in the other, and six had moderate loss in one eye and mild loss in the other. Many patients had undergone successful glaucoma surgery in either or both eyes to stabilize intraocular pressure bilaterally.[22]

The mean intraocular pressure among participants in the present study was 14.98 ± 0.9 mm Hg in the right eye and 13.95 ± 0.8 mm Hg in the left. Only 17% of subjects were receiving any topical ocular hypotensive therapy in either eye with the clinical intent of enhancing intraocular pressure (IOP) reduction. No oral ocular hypotensive agent was in use by

Table 1. Mean Right and Left Eye FDT 30-2 MD and PSD Global Index Values (MD and PSD from the Perimetry Printouts) With Associated SEs for All Right and Left Eyes of Consecutive Patients With Clinically Stabilized Bilateral Moderate to Severe VF Loss ($n = 41$)

Full Data Set		Right Eye	Left Eye
($n = 41$)	Mean of FDT MD values (SEM)	−10.89 (0.8)	−11.16 (0.84)
	Mean FDT PSD value (SEM)	6.2 (0.28)	5.24 (0.24)

Table 2. Age, Gender, and Right and Left Eye MD and PSD Values for the 41 Subjects, Confirming the Bilateral Severity of the FDT 30-2 VF Loss Among the Study Population

	Age	Sex	Right Eye MD	Right Eye PSD	Left Eye MD	Left Eye PSD
1	19	Female	−8.74	4.88	−8.63	6.28
2	36	Female	−16.6	5.89	−20.03	4.88
3	43	Female	−5.01	3.59	−3.26	3.46
4	50	Female	−4.04	4.69	−5.58	5.38
5	58	Male	−11.35	6.36	−15.92	5.92
6	59	Female	−5.53	4.72	−8.24	4.51
7	59	Female	−4.47	4.04	−7.04	3.6
8	60	Female	−8.22	6.02	−6.38	5.74
9	60	Male	−13.87	8.85	−16.79	7.38
10	62	Female	−12.94	6.14	−7.3	4.73
11	62	Female	−16.86	5.35	−13.44	6
12	64	Male	−4.99	5.73	−8.5	6.52
13	67	Male	−3.36	4.55	−8.68	6.4
14	67	Male	−9.12	5.29	−11.29	7.45
15	68	Female	−6.17	6.31	−7.7	7.21
16	68	Female	−18.18	10.27	−15.28	7.02
17	69	Female	−9.39	5.28	−10.14	5.19
18	69	Male	−11.27	4.41	−15.78	4.62
19	70	Female	−10.9	7	−14.79	8.63
20	71	Female	−3.03	3.79	−8.96	5.09
21	71	Female	−14.08	6.91	−12.5	7.8
22	71	Female	−17.93	8.07	−16.21	7
23	72	Female	−6.15	3.5	−3.09	3.73
24	72	Male	−20.41	5.08	−19.91	5.85
25	72	Female	−12.79	8.35	−21.21	6.76
26	73	Male	−19.45	8.93	−21.24	7.48
27	73	Female	−9.55	6.22	−4.87	4.11
28	75	Female	−2.12	3.58	−3.22	4.25
29	75	Female	−20.18	7.86	−9.76	7.41
30	78	Female	−14.04	10.91	−9.39	8.22
31	79	Female	−8.7	8.8	−13.39	6.07
32	79	Female	−18.49	7.82	−22.26	4.32
33	79	Female	−9.33	7.32	−11.61	9.75
34	79	Male	−18.12	5.42	−17.85	4.97
35	81	Female	−6.6	7.75	−7.57	5.34
36	83	Female	−10.42	6.34	−9.9	6.91
37	84	Male	−10.44	5.74	−7.6	4.38
38	84	Male	−8.04	5.58	−11.64	4.79
39	85	Female	−11.39	7.08	−4.17	4.19
40	89	Female	−10.78	5.21	−5.31	2.97
41	93	Female	−13.27	4.55	−11.01	4.97

any subject. Twelve percent of subjects were only prescribed topical carbonic anhydrase inhibitor (CAI) eye drops with the intent of augmenting ocular vascular perfusion.[23] Twenty-seven percent of the subjects were receiving a combination of topical CAI with a topical ocular hypotensive agent.

Figure 2 shows examples of paired VFs with inverse tendency for focal field loss. Note the

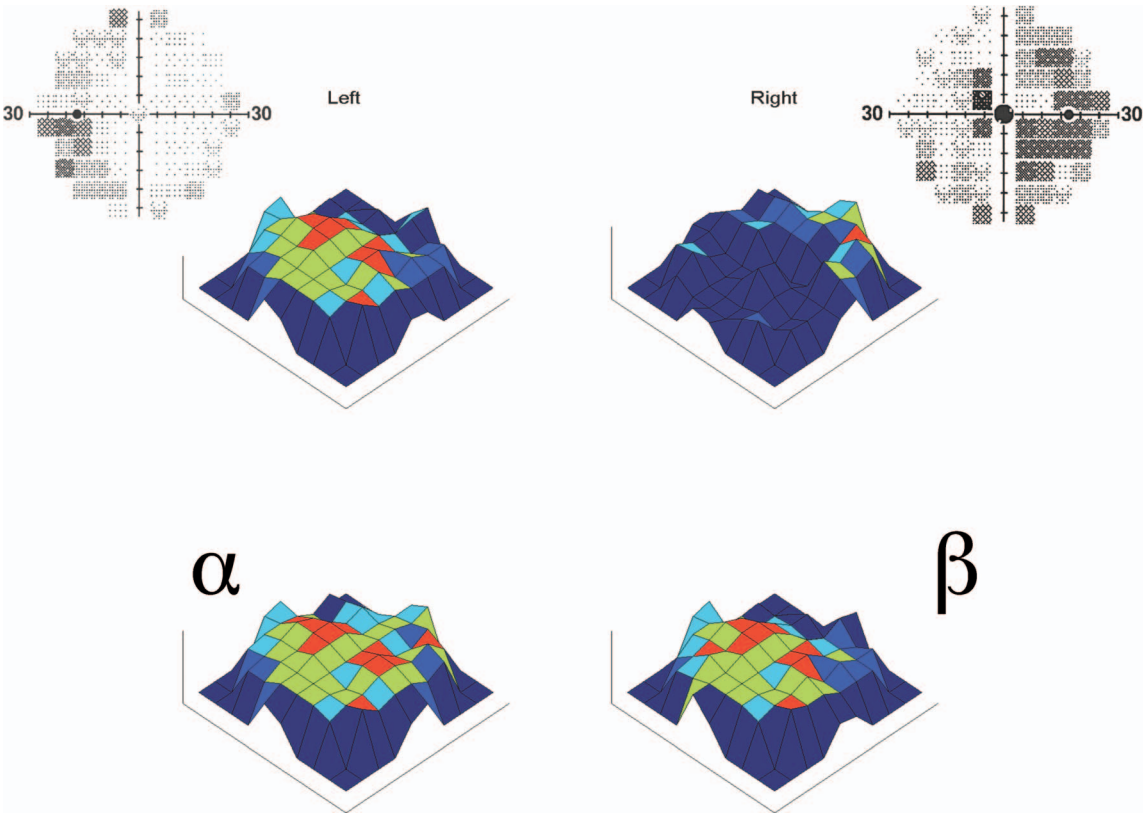

Figure 3. Example of pairing algorithm outcomes and associated 3-D heat maps. Left and right FDT 30-2 VF pair for one subject (gray-scale 2-D, *above*) and associated set of heat maps (colored 3-D, *below*). Note that the lower left composite applying the better of each of the 69 loci (α) arising naturally for the two eyes has a much less pathologic binocular VF loss than the composite derived from isopterically equivalent randomly selected points (β) at the lower right. The probability that the mean logarithmic global light sensitivity threshold was the same for pairings (α) and (β) among all 41 subjects was $< 10^{-9}$. The mean global threshold for (α) was 20.9 and for (β) 19.5 decibels.

alternating positive and negative complementarity between the right and left VFs results in a much more normal binocular field than would be predicted by chance. Other individuals in the study had significant loss in the same quadrant or hemifield in both eyes, making bilateral compensatory effects far less obvious on cursory inspection of the fields; however, in all but one subject the natural pairing used to estimate the binocular field was better than could be explained by a random ordering of concomitant loci. All patients were included in the statistical analysis.

Figure 3 provides a 3-D projection heat map set for one specimen VF pair with results obtained by the actual natural focal pairings of all 69 FDT Matrix VF loci (α) and the mean of 10,000 randomized isopterically equivalent pairings using the same left eye VF data (β). The physiologically balanced pairings would render an improved but still severely defective binocular VF, while the natural pairings yielding an approximately normal binocular field.

Statistical analysis reaffirms the general strength of this tendency in the entire study population. Figure 4 and Table 3 illustrate and summarize the statistical findings from the full study group ($n = 41$; 82 eyes). Among these eyes, the mean threshold value across the entire VF (69 loci) was 17.0 dB for left eyes and 18.4 dB for right eyes (average 17.7), 4 dB lower than the binocular field formed by pairing concomitant loci (α) at 20.9 dB ($P < 10^{-12}$). This mean threshold value (α) for concomitant direct pairings was significantly higher than could be explained by randomization of co-isopterically equivalent loci (β), which yielded 19.5 dB ($P < 10^{-9}$). The natural bilateral overlay pairings (α) provided function levels within 0.4 dB of the mean of the very highest of the 41 individual results among the 690,000 randomized pairings used to calculate β values. Thus, the binocular Matrix VF was conserved much better than could be explained by random chance. Mirrored symmetric pairings of contralateral concom-

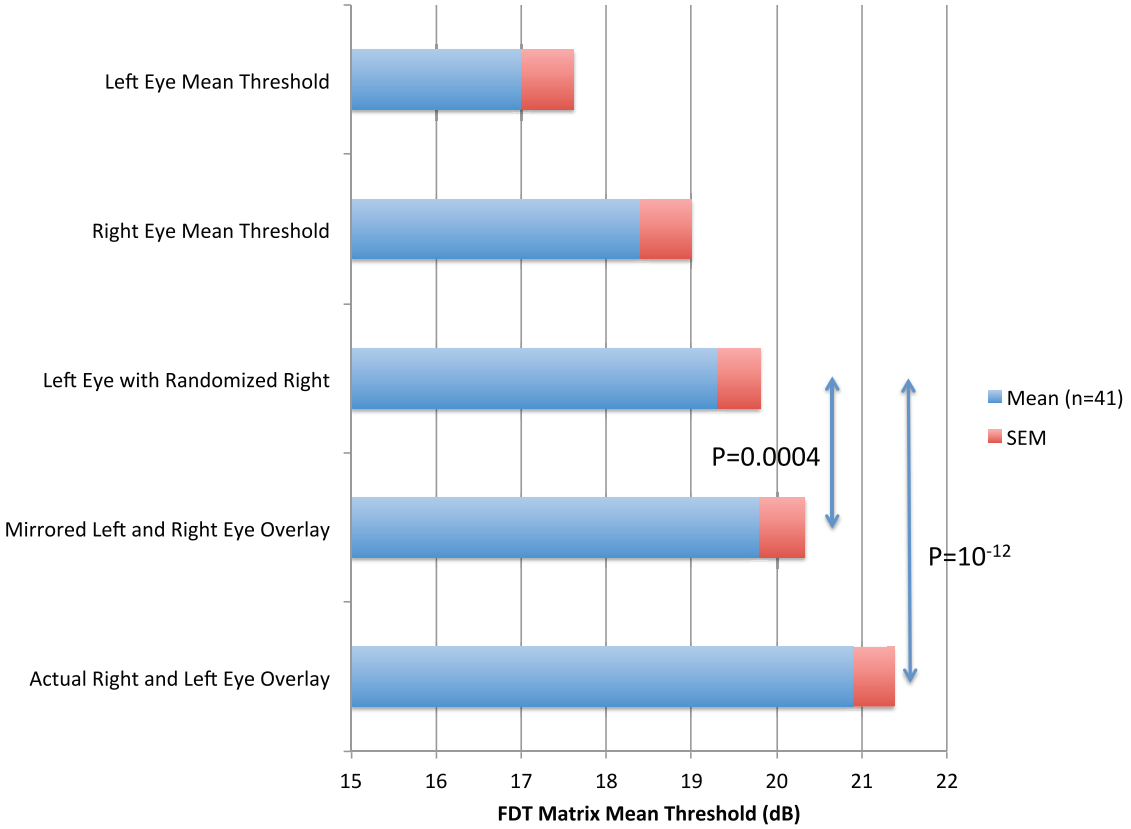

Figure 4. Mean thresholds for monocular and paired VF outcomes. Histogram showing global mean FDT Matrix threshold values ($n = 41$) with associated SEMs for left (a) and right eye (b) FDT 30-2 VFs, and for both eyes overlying the higher of the 69 concomitant right and left eye using: (c) the pairings of each left eye locus with any alternate randomly selected co-isopteric right eye values (repeated for all 69 loci $\times$ 10,000 iterations for each of the 41 eyes), (d) for each left eye locus with its precise mirror-image symmetric locus, and (e) the natural concomitant right and left eye pairings. The actual observed fields provide the highest conjoint sensitivity.

Table 3. Comparative Mean Threshold Differences and Associated Paired *t*-Test *P* Values for Consecutive Patients, Comparing Mean Threshold Compilations From Right and Left Eye FDT 30-2 Full Threshold VFs ($N = 41$)

	Randomized Bilateral Mean Threshold (*P* Value)	Mirrored Bilateral Threshold (*P* Value)	Overlayed Bilateral Mean Threshold (*P* Value)	Best of 10,000 Random Pairings (*P* Value)
Left eye mean threshold	−7.46 dB* ($<10^{-8}$)	−9.96 dB* ($<10^{-11}$)	−10.68 dB* ($<10^{-12}$)	−9.33 dB* ($<10^{-10}$)
Right eye mean threshold	−2.84 dB* (0.007)	−6.96 dB* ($<10^{-7}$)	−7.96 dB* ($<10^{-9}$)	−4.91 dB* ($<10^{-4}$)
Randomized bilateral mean threshold		−6.62 dB* ($<10^{-7}$)	−8.58 dB* ($<10^{-9}$)	−11.88 dB* ($<10^{-13}$)
Mirrored bilateral threshold			−3.91 dB* (0.0003)	0.77 dB (0.446)
Overlayed bilateral mean threshold				2.9 dB* (0.006)

* Indicates significant values $P < 0.05$.

itant loci also produced values higher than random co-isopteric pairings (Δ 1 dB; $t = -6.6$; $P < 10^{-7}$).

Evaluation of the central loci within a vertically oriented ellipse indicated the strong influence of symmetry: the mirrored fields were on average 1 dB better than could be expected by chance ($P < 0.0001$). The true field was only better than this mirrored field by 0.3 dB ($P = 0.009$). These findings were very different from the same comparison performed on loci falling outside this ellipse: the binocular field found using the mirrored left eye was not significantly better than could be expected by chance ($P = 0.08$), but the true binocular field was 0.6 dB better than the mirrored binocular field ($P < 0.0001$). This finding indicates that some symmetric process may play a role in preserving the central portion of the binocular field, but that it is not active in the peripheral field.

If there were a simple anatomic ocular symmetry compensation, the mirror-image pairings would actually be expected to be significantly worse than random, quantitatively opposite to the highly significant positive transcortical relationship we observed. This appears to reflect the +/− concentric intra-hemispheric and trans-hemispheric complementarity that exist for right and left eye spatial projections to the striate cortex (see Figure 1).

Discussion

Analysis of these Matrix fields confirms our previous finding of a strong tendency to conserve the binocular field in late-stage glaucoma.[4] This conservation cannot be explained by chance or symmetry, thereby apparently implicating a symmetry-breaking process by which contralateral fields are found to be complementary.

Some data suggest interaction between the cortex and SC in governing binocular vision in primates[24,25] and humans.[26,27] Dieback appears early on in the SC[5,6] and interconnectivity between SCs may coordinate patency of the binocular VF across the vertical meridian.[28,29]

The thalamic lateral geniculate is a bilateral structure that includes six layers: layers 2, 3, and 5 receive information from the ipsilateral eye while layers 1, 4, and 6 from the contralateral eye. Close proximity of bilaterally derived information in this structure makes it a likely candidate for coordinating VF preservation. Locations in adjacent layers correspond to visually concomitant areas of each retina. It has been shown that when there is damage to one optic nerve, compensatorily higher light sensitivity is developed to adjacent layer input in the lateral geniculate from the fellow eye.[30] Focal axonal injury in one eye appears to be accompanied by increased activity in the contralateral retinal glia and geniculate layers receiving concomitant visual information from the fellow noninjured eye.[30–32] One factor could be that adjacent geniculate layers share the same vascular supply, so loss of axons from one eye may be accompanied by increased availability of nutrients to, and more rapid clearance of catabolites from, the immediately adjacent contralateral eye synapses. Focally coordinated bilateral compensation of this kind may play a role in the conservation of the binocular VF in patients with chronic progressive glaucoma. Whether some neuroprotective or neuroplastic regenerative feature is involved remains to be determined. Identification of regulatory mechanisms might suggest new treatment options.

The finding of the opposite symmetry in the central field may be a side effect of trans-collosal connections that reinforce bilateral symmetry.[15] The portion of the field involved in computation of bilateral symmetry grows in inverse proportion to the stimuli used.[13,14] This different wiring of the central field for low spatial frequency stimuli might mean different fates in glaucoma for cells sensitive to low spatial frequencies. We did not observe this reversed jigsaw effect centrally in SAP fields.[4] However, the very small (high spatial frequency) SAP stimuli would not be expected to stimulate symmetry pathways outside the central 6 degrees. Tests with 10-2 test patterns, or smaller, might reveal a similar reverse-jigsaw effect centrally. In any case, the possibility of connectivity between V2 regions determining the fate of glaucomatous VFs perhaps boosts the case for more cortical involvement than SC in primate glaucoma.

The size of complementary scotomata may be related to the width of the ocular dominance column projected into visual space (Fig. 1). This may limit binocular interaction for any mechanism based on cortical plasticity.

It is important to re-emphasize that many investigations on apparent anterograde CNS associations with optic neuropathy[33–42] preceded the landmark Vanderbilt laboratory studies showing the progression of chronic glaucoma proceeds in a retrograde fashion from brain to eye.[5] We previously demonstrated a tendency of late-stage glaucoma patients' paired fields to maintain binocular complementarity at a level far exceeding what might be explained by chance.[4] The present study comprises additional clinical evidence of brain involvement in coordinating

binocular ganglion cell function and viability to maximize the binocular VF in patients with advanced chronic glaucoma.

As mentioned in our previous article, this data may offer new insights into Alzheimer's disease, which, like chronic glaucoma, is an age-related neurodegenerative disorder.[43–46] Both are progressive diseases involving symmetric bilateral structures within which neurodegeneration proceeds in an asymmetric fashion. It therefore seems possible that analogous symmetry-breaking conservation mechanisms may be involved. Paired eyes provide an ideal, statistically powerful system for the evaluation of placebo-controlled, intrasubject CNS studies without regard for the confounding effects of intersubject variability.[47] Perhaps the additional information yielded in the present study demonstrating the unexpected converse compensatory effects associated with spatial symmetry within the VF may further assist in the elucidation of the brain's integrated involvement in progressive age-related neurodegenerations.

Our prior work with SAP in patients with advanced glaucoma did not address the possibility that CNS control might be in play in patients with milder disease. The present study incorporates a high proportion of eyes with mild and moderate VF loss, and reaffirms that the jigsaw effect takes hold early on in chronic glaucoma. Detection of such bilateral compensation at a subclinical stage might facilitate the early characterization and timely treatment of chronic glaucoma before more severe permanent neuronal damage can occur.

Our prior SAP study included simultaneous bilateral testing of both eyes of an arbitrary subset of patients, confirming that the higher of the two attenuation threshold values for each paired locus in the individual right and left Humphrey 30-2 VFs was indeed the value obtained in the binocular field. The FDT Matrix device is not designed in a manner that would allow for simultaneous testing of both eyes. However, a more advanced device that would readily allow for such testing is in development, and extensive testing on prototypes has been published.[48,49] Once available, such testing methods may help better define actual functional visual disability and more accurately reflect the functional efficacy of current ocular and future CNS-oriented therapeutic approaches, even in patients with relatively mild disease.

Acknowledgments

All authors contributed significantly to the preparation of this manuscript. William Eric Sponsel devised the concept for the paper. Analaura Villarreal gathered the visual fields and Analaura Villarreal, William Eric Sponsel, and Matthew A. Reilly all input the data. Matthew A. Reilly ran the statistical analysis of the field data. Matthew A. Reilly, William Eric Sponsel, and Analaura Villarreal created the graphs and figures. The draft manuscript was written by William Eric Sponsel and Matthew A. Reilly, with subsequent additions, revisions, and editing by all the co-authors. Ted Maddess and William Eric Sponsel performed literature searches.

William Eric Sponsel is a Primary Investigator in the Australian Research Council Centre of Excellence in Visual Sciences, of which co-author Ted Maddess is Director.

Disclosure: **M.A. Reilly**, None; **A. Villarreal**, None; **T. Maddess**, previously received royalities for sale of the FDT/Matrix perimeters (Carl Zeiss Meditec AG) and holds patents on the device mentioned in the references 48 and 49 (nuCoria Pty Ltd); **W.E. Sponsel**, None

References

1. Caprioli J. Automated perimetry in glaucoma. In: Walsh TJ, ed. *Visual Fields: Examination and Interpretation*. San Francisco, CA: American Academy of Ophthalmology; 1990:71–105.
2. Ferreira SM, Lerner SF, Brunzini R, Evelson PA, Llesuy SF. Oxidative stress markers in aqueous humor of glaucoma patients. *Am J Ophthalmol*. 2004;137:62–69.
3. Kumar DM, Agarwal N. Oxidative stress in glaucoma: a burden of evidence. *J Glaucoma*. 2007;16:334–343.
4. Sponsel WE, Groth SL, Satsangi N, Maddess T, Reilly MA. Refined data analysis provides clinical evidence for central nervous system control of chronic glaucomatous neurodegeneration. *Transl Vis Sci Tech*. 2014;3:1.
5. Crish SD, Sappington RM, Inman DM, Horner PJ, Calkins DJ. Distal axonopathy with structural persistence in glaucomatous neurodegeneration. *Proc Nat Acad Sci*. 2010;107:5196–5201.
6. Schlamp CL, Li Y, Dietz JA, Janssen KT, Nickells RW. Progressive ganglion cell loss and optic nerve degeneration in DBA/2J mice is

variable and asymmetric. *BMC Neurosci*. 2006;7:66.
7. Weber AJ, Chen H, Hubbard WC, Kaufman PL. Experimental glaucoma and cell size, density, and number in the primate lateral geniculate nucleus. *Invest Ophthalmol Vis Sci*. 2000;41:1370–1379.
8. Yucel YH, Zhang Q, Gupta N, Kaufman PL, Weinreb RN. Loss of neurons in magnocellular and parvocellular layers of the lateral geniculate nucleus in glaucoma. *Arch Ophthalmol*. 2000;118:378–384.
9. Yucel YH, Zhang Q, Weinreb RN, Kaufman PL, Gupta N. Atrophy of relay neurons in magno- and parvocellular layers in the lateral geniculate nucleus in experimental glaucoma. *Invest Ophthalmol Vis Sci*. 2001;42:3216–3222.
10. Calkins DJ. Critical pathogenic events underlying progression of neurodegeneration in glaucoma. *Prog Retinal Eye Res*. 2012;31:702–719.
11. Calkins DJ. Age-related changes in the visual pathways: blame it on the axon. *Invest Ophthalmol Vis Sci*. 2013;(54);ORSF37-41.
12. Adams DL, Sincich LC, Horton JC. Complete pattern of ocular dominance columns in human primary visual cortex. *J Neurosci*. 2007;27:10391–10403.
13. Dakin SC, Herbert AM. The spatial region of integration for visual symmetry detection. *Proc Biol Sciences*. 1998;265:659–664.
14. Rainville SJ, Kingdom FA. Scale invariance is driven by stimulus density. *Vis Res*. 2002;42:351–367.
15. Abel P, O'brien B, Olavarria J. Organization of callosal linkages in visual area V2 of macaque monkey. *J Comp Neurol*. 2000;428:278–293.
16. Rosli Y, Maddess T, Bedford SM. Low spatial frequency channels and the spatial frequency doubling illusion. *Invest Ophthalmol Vis Sci*. 2009;50:1956–1963.
17. Bengtsson B, Olsson J, Heijl A, Rootzen H. A new generation of algorithms for computerized threshold perimetry, SITA. *Acta Ophthalmol*. 1997;75:368–375.
18. Budenz DL, Rhee P, Feuer WJ, McSoley J, Johnson CA, Anderson DR. Comparison of glaucomatous visual field defects using standard full threshold and Swedish interactive threshold algorithms. *Arch Ophthalmol*. 2002;120:1136–1141.
19. Sponsel WE, Arango S, Trigo Y, Mensah J. Clinical classification of glaucomatous visual field loss by frequency doubling perimetry. *Am J Ophthalmol*. 1998;125:830–836.
20. Sponsel WE, Ritch R, Stamper R, et al. Prevent Blindness America visual field screening study. The Prevent Blindness America Glaucoma Advisory Committee. *Am J Ophthalmol*. 1995;120:699–708.
21. Crabb DP, Viswanathan AC, McNaught AI, Poinoosawmy D, Fitzke FW, Hitchings RA. Simulating binocular visual field status in glaucoma. *Brit J Ophthalmol*. 1998;82:1236–1241.
22. Sponsel WE, Groth SL. Mitomycin-augmented non-penetrating deep sclerectomy: preoperative gonioscopy and postoperative perimetric, tonometric and medication trends. *Brit J Ophthalmol*. 2013;97:357–361.
23. Sponsel WE, Harrison J, Elliott WR, Trigo Y, Kavanagh J, Harris A. Dorzolamide hydrochloride and visual function in normal eyes. *Am J Ophthalmol*. 1997;123:759–766.
24. Cynader M, Berman N. Receptive-field organization of monkey superior colliculus. *J Neurophys*. 1972;35:187–201.
25. Lane RH, Allman JM, Kaas JH, Miezin FM. The visuotopic organization of the superior colliculus of the owl monkey (Aotus trivirgatus) and the bush baby (Galago senegalensis). *Brain Res*. 1973;60:335–349.
26. DuBois RM, Cohen MS. Spatiotopic organization in human superior colliculus observed with fMRI. *Neuroimage*. 2000;12:63–70.
27. Limbrick-Oldfield EH, Brooks JC, Wise RJ, et al. Identification and characterisation of midbrain nuclei using optimised functional magnetic resonance imaging. *Neuroimage*. 2012;59:1230–1238.
28. Tardif E, Clarke S. Commissural connections of human superior colliculus. *Neurosci*. 2002;111:363–372.
29. Knudsen EI. Control from below: the role of a midbrain network in spatial attention. *Eur J Neurosci*. 2011;33:1961–1972.
30. Luthra A, Gupta N, Kaufman PL, Weinreb RN, Yucel YH. Oxidative injury by peroxynitrite in neural and vascular tissue of the lateral geniculate nucleus in experimental glaucoma. *Exp Eye Res*. 2005;80:43–49.
31. Bodeutsch N, Siebert H, Dermon C, Thanos S. Unilateral injury to the adult rat optic nerve causes multiple cellular responses in the contralateral site. *J Neurobiol*. 1999;38:116–128.
32. Yucel Y, Gupta N. Glaucoma of the brain: a disease model for the study of transsynaptic neural degeneration. *Prog Brain Res*. 2008;173:465–478.
33. Dai Y, Sun X, Chen Q. Differential induction of c-Fos and c-Jun in the lateral geniculate nucleus

of rats following unilateral optic nerve injury with contralateral retinal blockade. *Exp Brain Res (Experimentelle Hirnforschung Experimentation cerebrale)*. 2009;193:9–18.
34. Macharadze T, Goldschmidt J, Marunde M, et al. Interretinal transduction of injury signals after unilateral optic nerve crush. *Neuroreport*. 2009; 20:301–305.
35. Morgan JE, Uchida H, Caprioli J. Retinal ganglion cell death in experimental glaucoma. *Brit J Ophthalmol*. 2000;84:303–310.
36. Panagis L, Thanos S, Fischer D, Dermon CR. Unilateral optic nerve crush induces bilateral retinal glial cell proliferation. *Eur J Neuroscience*. 2005;21:2305–2309.
37. Weber AJ, Kaufman PL, Hubbard WC. Morphology of single ganglion cells in the glaucomatous primate retina. *Invest Ophthalmol Vis Sci*. 1998;39:2304–2320.
38. Caleo M, Menna E, Chierzi S, Cenni MC, Maffei L. Brain-derived neurotrophic factor is an anterograde survival factor in the rat visual system. *Curr Biol*. 2000;10:1155–1161.
39. Martin KR, Quigley HA, Zack DJ, et al. Gene therapy with brain-derived neurotrophic factor as a protection: retinal ganglion cells in a rat glaucoma model. *Invest Ophthalmol Vis Sci*. 2003;44:4357–4365.
40. Matthews MR. Further observations on transneuronal degeneration in the lateral geniculate nucleus of the macaque monkey. *J Anat*. 1964;98: 255–263.
41. Riddle DR, Lo DC, Katz LC. NT-4-mediated rescue of lateral geniculate neurons from effects of monocular deprivation. *Nature*. 1995;378:189–191.
42. Yucel YH, Kalichman MW, Mizisin AP, Powell HC, Weinreb RN. Histomorphometric analysis of optic nerve changes in experimental glaucoma. *J Glaucoma*. 1999;8:38–45.
43. Frost SM, Kanagasingam Y, Sohrabi HR, et al. Pupil response biomarkers distinguish amyloid precursor protein mutation carriers from non-carriers. *Curr Alzheimer Res*. 2013;10:790–796.
44. McKinnon SJ. Glaucoma: ocular Alzheimer's disease? *Frontiers Biosci*. 2003;8:s1140–s1156.
45. Mungas D, Harvey D, Reed BR, et al. Longitudinal volumetric MRI change and rate of cognitive decline. *Neurology*. 2005;65:565–571.
46. Patton N, Aslam T, Macgillivray T, Pattie A, Deary IJ, Dhillon B. Retinal vascular image analysis as a potential screening tool for cerebrovascular disease: a rationale based on homology between cerebral and retinal microvasculatures. *J Anat*. 2005;206:319–348.
47. Sponsel W, McKinnon S. Preface; Special Edition; Neuroprotection and the Eye. *Brain Res Bull*. 2004;62:435–437.
48. Maddess T, Bedford SM, Goh XL, James AC. Multifocal pupillographic visual field testing in glaucoma. *Clin Exp Ophthalmol*. 2009;37:678–686.
49. Carle CF, James AC, Kolic M, Loh YW, Maddess T. High-resolution multifocal pupillographic objective perimetry in glaucoma. *Invest Ophthalmol Vis Sci*. 2011;20:336–343.